JOURNAL OF COMPUTATIONAL PHYSICS 66, 62–82 (1986)

A Nearly-Implicit Hydrodynamic Numerical Scheme for Two-Phase Flows*

JOHN A. TRAPP

Department of Mechanical Engineering, University of Colorado, Denver, Colorado 80202

AND

RICHARD A. RIEMKE

EG&G Idaho, Inc., Idaho National Engineering Laboratory, Idaho Falls, Idaho 83415

Received June 5, 1985; revised October 11, 1985

This article presents an extension of the semi-implicit numerical scheme for two-phase flow simulation. The extension uses an implicit evaluation of the convective fluxes and thus eliminates the material Courant stability restriction. The new algorithm involves a two-step approach for the mass and energy equations and a single fully-implicit step for the momentum evaluations. Some analysis and accuracy considerations for the scheme are also presented.

1. INTRODUCTION

Complex two-phase flows have been numerically simulated in the nuclear industry for over a decade. The major numerical schemes used to analyze the total system response of nuclear power plants until recently have been based upon semi-implicit finite difference schemes [1–4]. A more implicit numerical scheme called SETS [5] has been implemented in the systems code TRAC–PF1 [6]. RELAP5 (Reactor Excursion and Leak Analysis Program) is one such semi-implicit systems code. The basic guidelines employed in the development of the semi-implicit numerical scheme are discussed in Ref. [4]. The resulting semi-implicit scheme has the interphase drag, heat transfer, and mass transfer terms evaluated implicitly (in linear fashion) to eliminate the small time step restrictions associated with the short time constants of the interphase exchange processes. In addition, the terms responsible for acoustic pressure wave propagation—the convective velocities in the mass and energy conservation equations and the pressure gradient in the momentum

* Work supported by the U. S. Nuclear Regulatory Commission, Office of Nuclear Regulatory Research under U. S. Department of Energy Contract DE-AC07-76ID01570.

0021-9991/86 $3.00

equations—are evaluated at the new time $(n+1)$ level. This semi-implicit scheme has a time step restricted by the material Courant limit ($\Delta t \leqslant \Delta x/v_g$, $\Delta t \leqslant \Delta x/v_f$) because the convected fluxes of mass, energy, and momentum are all evaluated with old time (n) level values.

The semi-implicit scheme was designed at a time when there was much emphasis on large break loss-of-coolant accident (LOCA) analysis. In these simulations there is little need to follow dynamic acoustic wave propagation, except possibly for the first few milliseconds. The dynamic material transport of mass and energy through the system is important and accuracy alone dictates a time step less than the material Courant limit. For this reason there was no incentive to expend the extra calculational effort required to evaluate the convective fluxes implicitly, and eliminate the material Courant time step stability restriction. As the emphasis has expanded to include very slow transients that require hours or days of real time simulation, the numerical schemes have been reexamined. If the *dynamic* propagation of mass and energy is not important, then the convectively fluxed variables could be evaluated implicitly to eliminate the material Courant time step restriction. This has been the goal in the numerical scheme development described in this article. One such prior scheme has been described in the literature [7, 5] and we have profited from these works. The present scheme differs from the above in the amount of implicitness used for the momentum evaluations. The prior scheme used multistep evaluations of both the momentum and energy equations. The present scheme uses a two-step evaluation of the mass and energy equations but a single fully-implicit step for the momentum equations. The new scheme, referred to as the nearly-implicit scheme, has the convective fluxes evaluated implicitly, and hence eliminates the material Courant time step stability restriction. During the review process for this paper, the authors became aware of the ATHENA system code developed in Canada [8]. This two-fluid code is more implicit than all of the prior efforts. The convective flux terms are evaluated implicitly in a single step. A comparison for the run times of each of these schemes will be given later.

If a numerical simulation is for a basically quasi-steady process with slowly-varying boundary conditions, this scheme will allow a large time step and still give sufficiently accurate predictions. It is this class of problems for which the nearly-implicit scheme is primarily developed. In addition, it will give a very fast and efficient way to establish steady-state initial conditions. If this scheme is used with a time step slightly larger than the material Courant limit, the calculation still gives accurate simulations for problems with dynamic convection of mass and energy. If a time step significantly larger than the material Courant limit is used (5 to 10 times larger), *dynamic* propagation of mass, energy, and void is filtered out by the numerical simulation. This point will be expanded upon later.

Clearly, then, the new solution scheme will not be universally applicable across the broad range of reactor transients of interest. Additional work will be required to implement automatic controls or to specify detailed guidelines for using the new scheme. In any event, the nearly-implicit solution scheme promises to offer substantial savings in computer time for many transients of interest.

Section 2 of this article describes the basic two-fluid equations used in a one-dimensional two-phase flow analysis. Section 3 provides a theoretical background for the nearly-implicit scheme by examining the effect of implicit solutions and time step size on short wavelength behavior. Section 4 describes the nearly-implicit scheme implemented in RELAP5 and contrasts it with the existing semi-implicit scheme. Section 5 considers accuracy limitations of the new scheme. Section 6 presents the results of three simple test problems used to evaluate the nearly-implicit scheme and to compare it to the semi-implicit scheme. Section 7 is a summary.

2. Basic Two-Fluid Model

The basic field equations for the two-fluid nonequilibrium model consists of two phasic continuity equations, two phasic momentum equations, and two phasic energy equations. The equations are recorded in differential form with time and one space dimension as independent variables and in terms of time and volume-average dependent variables. The development of such equations for the two-phase process has been recorded in Ref. [9] and is not repeated here.

The phasic continuity equations are

$$\frac{\partial}{\partial t}(\alpha_g \rho_g) + \frac{\partial}{\partial x}(\alpha_g \rho_g v_g) = \Gamma_g \tag{1}$$

and

$$\frac{\partial}{\partial t}(\alpha_f \rho_f) + \frac{\partial}{\partial x}(\alpha_f \rho_f v_f) = -\Gamma_g. \tag{2}$$

The phasic momentum equations are

$$\alpha_g \rho_g \frac{\partial v_g}{\partial t} + \frac{1}{2}\alpha_g \rho_g \frac{\partial v_g^2}{\partial x} = -\alpha_g \frac{\partial P}{\partial x} + \alpha_g \rho_g B - \alpha_g \rho_g F_{wg} v_g - \alpha_g \alpha_f \rho_g \rho_f F_i (v_g - v_f) \tag{3}$$

and

$$\alpha_f \rho_f \frac{\partial v_f}{\partial t} + \frac{1}{2}\alpha_f \rho_f \frac{\partial v_f^2}{\partial x} = -\alpha_f \frac{\partial P}{\partial x} + \alpha_f \rho_f B - \alpha_f \rho_f F_{wf} v_f - \alpha_g \alpha_f \rho_g \rho_f F_i (v_f - v_g). \tag{4}$$

The phasic energy equations are

$$\frac{\partial}{\partial t}(\alpha_g \rho_g U_g) + \frac{\partial}{\partial x}(\alpha_g \rho_g U_g v_g) = -P\frac{\partial \alpha_g}{\partial t} - P\frac{\partial}{\partial x}(\alpha_g v_g) + Q_{wg} + Q_{ig} + \Gamma_g h_g^* \tag{5}$$

and

$$\frac{\partial}{\partial t}(\alpha_f \rho_f U_f) + \frac{\partial}{\partial x}(\alpha_f \rho_f U_f v_f) = -P\frac{\partial \alpha_f}{\partial t} - P\frac{\partial}{\partial x}(\alpha_f v_f) + Q_{wf} + Q_{if} - \Gamma_g h_f^*. \tag{6}$$

In Eqs. (1) through (6) the g and f subscripts refer to the gas and liquid phases, respectively. The nomenclature is as follows: α is the volume void fraction, ρ is the phasic density, v is the phasic velocity, P is the common pressure, U is the phasic internal energy, h is the phasic enthalpy, Q_w represents the wall heart flux, F_w represents the wall drag, Γ is the interphase mass exchange, Q_i is the interphase heat exchange, F_i is the interphase drag force, and B represents the body forces (usually gravity).

The enthalpies associated with interphase mass transfer Γ_g in Eqs. (5) and (6) are defined in such a way that the interface energy jump conditions at the liquid–vapor interface are satisfied. In particular, h_g^* and h_f^* are chosen to be h_g^s and h_f, respectively, for the case of vaporization and h_g and h_f^s, respectively, for the case of condensation. A superscript s denotes a saturation value. The interphase energy transfer terms Q_{ig} and Q_{if} can be expressed as

$$Q_{ig} = H_{ig}(T^s - T_g) \tag{7}$$

and

$$Q_{if} = H_{if}(T^s - T_f). \tag{8}$$

H_{ig} and H_{if} are the heat transfer coefficients from the interface, which is assumed to be at the saturation condition, to the vapor and liquid phases, respectively. T^s, T_g, and T_f are the saturation temperature, vapor temperature, and liquid temperature, respectively. The interphase vaporization (or condensation) rate is obtained from the energy jump condition as

$$\Gamma_g = -\frac{Q_{ig} + Q_{if}}{h_g^* - h_f^*} \tag{9}$$

which, upon substitution of Eqs. (7) and (8), becomes

$$\Gamma_g = -\frac{H_{ig}(T^s - T_g) + H_{if}(T^s - T_f)}{h_g^* - h_f^*}. \tag{10}$$

The phase change process which occurs at the interface is envisioned as a process in which bulk fluid is heated or cooled to the saturation temperature, and phase change occurs at the saturation state.

In the momentum Eqs. (3) and (4), two terms included in these basic equations have not been shown. The virtual mass terms that describe the inertial coupling of

the phases in accelerating flows are included but not recorded in Eqs. (3) and (4). In addition, the momentum equations include a term (a spatial gradient of the void fraction) describing the effects of a transverse gravity head in a horizontal flow situation, which has not been recorded in Eqs. (3) and (4). These two terms are not of any fundamental significance to the nearly-implicit scheme and for the simplicity of this presentation are not discussed in what follows. As the momentum equations are fully coupled, these terms cause no complications in the nearly-implicit scheme.

It has proven useful in the degenerate case of an equal velocity model to use the momentum equations as a sum and difference of the liquid and vapor momentum equations. Adding Eqs. (3) and (4) gives the resulting sum equation

$$\alpha_g \rho_g \frac{\partial v_g}{\partial t} + \alpha_f \rho_f \frac{\partial v_f}{\partial t} + \frac{1}{2}\alpha_g \rho_g \frac{\partial v_g^2}{\partial x} + \frac{1}{2}\alpha_f \rho_f \frac{\partial v_f^2}{\partial x} = -\frac{\partial P}{\partial x} + \rho B$$
$$-\alpha_g \rho_g F_{wg} v_g - \alpha_f \rho_f F_{wf} v_f. \tag{11}$$

Dividing Eq. (4) by $\alpha_f \rho_f$ and subtracting it from Eq. (3) divided by $\alpha_g \rho_g$ gives the resulting difference equation

$$\frac{\partial v_g}{\partial t} - \frac{\partial v_f}{\partial t} + \frac{1}{2}\frac{\partial v_g^2}{\partial x} - \frac{1}{2}\frac{\partial v_f^2}{\partial x} = -\left(\frac{1}{\rho_g} - \frac{1}{\rho_f}\right)\frac{\partial P}{\partial x} - F_{wg} v_g + F_{wf} v_f$$
$$-\rho F_i (v_g - v_f). \tag{12}$$

Equations (11) and (12) are used in the numerical model as momentum equations equivalent to Eqs. (3) and (4).

3. Preliminary Analysis

In the development of a numerical solution scheme for a system of partial differential equations, the time constants and/or propagation speeds associated with the simulated physical processes must be known. If it is desired to accurately follow all of the physical phenomena described by the differential equations, then the numerical simulation must be carried out with a time step, Δt, less than the smallest time constant of the system and such that the Courant number based upon the fastest wave speed is less than one. With this choice for the time step, any stable explicit numerical scheme is acceptable; the use of an implicit or semi-implicit scheme is a disadvantage because the numerical scheme is unduly complicated.

A question that naturally arises is whether there is an advantage to be gained by using an implicit numerical scheme that is stable for time steps larger than the physical time constants, or so large that propagation occurs through more than one cell length, Δx, per time step. It is always possible to develop an implicit scheme that gives stable calculations for large time steps, but when this approach is used to simulate a physical process, the solution may suffer a loss of fidelity. In particular,

the physical phenomena with time constants greater than Δt and the wave phenomena with wave speeds less than $\Delta x/\Delta t$ will be adequately simulated, whereas the physical phenomena with time constants smaller than Δt and the wave phenomena with wave speeds larger than $\Delta x/\Delta t$ will be lost or filtered out by the numerical solution process. Thus, implicit schemes may be advantageous in problems where dynamic propagation phenomena are unimportant or the processes of interest occur slowly so that large time steps can be used without loss of accuracy.

To illustrate these concepts, consider the simple single equation model

$$\frac{\partial a}{\partial t} + u\frac{\partial a}{\partial x} = -\frac{a}{\tau} \tag{13}$$

for constant propagation speed, u, and relaxation time constant, τ. The fully-implicit numerical scheme for this model (using a centered spatial approximation) is

$$a_j^{n+1} - a_j^n + \frac{u\Delta t}{2\Delta x}(a_{j+1}^{n+1} - a_{j-1}^{n+1}) = -\frac{\Delta t}{\tau} a_j^{n+1}. \tag{14}$$

Assuming that this numerical equation holds in an infinite medium, the exact solution for a general Fourier component $a_j^n = a_0 e^{i(kj\Delta x - \omega n\Delta t)}$ is given by

$$a_j^{n+1} = \left(1 \Big/ \left[1 + \frac{\Delta t}{\tau} + i\frac{u\Delta t}{\Delta x}\sin(k\,\Delta x)\right]\right) a_j^n, \tag{15}$$

where k is the wavenumber ($= 2\pi/\lambda$) for a particular Fourier mode of wavelength λ. Consider the solution, Eq. (15), for a time step much larger than the relaxation time constant, i.e., for $\Delta t/\tau \gg 1$. In this situation, $\Delta t/\tau$ dominates the denominator, and in the limit of large Δt, Eq. (15) reduces to

$$a_j^{n+1} \approx 0 \tag{16}$$

for all wavelengths of practical interest. The exact solution of Eq. (13) for this case is a periodic wave travelling with speed u and decaying amplitude.

Equation (16) states that the exact decaying wave solution to the differential equation is numerically approximated as the zero solution for large Δt. This implicit scheme when used with a large Δt (relative to τ) gives the correct asymptotic solution as $t \to \infty$, i.e., the steady state solution having all wave propagation phenomena damped.

Now consider Eq. (13) with the right-hand side set to zero for a large Δt such that $\Delta x/\Delta t \ll u$. The exact solution in this case is a periodic wave propagating with speed u and without decay. For this case the Courant number, $u(\Delta t/\Delta x)$, is large, and we again obtain the solution given by Eq. (16) even though the differential equation simulated contains no decay mechanism. In this case, the undamped

dynamic wave propagation phenomena present in the differential system has been filtered out completely by the numerical solution. Here we see in simple fashion a characteristic feature of a numerical scheme that has certain wave propagation terms evaluated implicitly. If a large time step is used with such a scheme, the *dynamic* wave propagation is filtered out in the numerical simulation. It should be noted that if the wavelength is extremely long (small k) such that $u(\Delta t/\Delta x)\sin(k\,\Delta x)$ is still much less than one, then these long waves may be accurately represented, whereas the short waves are effectively filtered out of the calculation. In Table I, the wavelengths at which decay to one-half the initial amplitude occurs in 64 time steps are tabulated for a range of Courant numbers (a value for Δx equal to 0.5 m is assumed). Wavelengths shorter than those tabulated will decay even faster. For component sizes typical of light water reactors, it is clear that all dynamic wave propagation information is lost at Courant numbers greater than 10.

Summarizing these two examples, it can be stated that for an implicit numerical scheme, with the time step taken much larger than a physical time constant associated with a particular source term, ony the asymptotic steady-state solution is simulated. In addition, if Δt is such that the Courant number associated with a particular propagation phenomena is much larger than one, then the implicit numerical scheme filters out all dynamic wave motion associated with this characteristic velocity.

In a complicated system of differential equations, there may be several different wave speeds and/or time constants present. In this case, if the time constants and/or wave speeds are widely separated, it is possible to design a numerical scheme that is partially implicit in the terms responsible for *one* process. It is then possible to obtain quasi-steady or damped/filtered simulation for that particular physical phenomenon while obtaining an accurate simulation for processes with larger time constants or slower wave propagation speeds. At times this is very desirable. Such a partially-implicit numerical scheme can be used to simulate all of the physical phenomena present when run with a sufficiently small time step, but it can also be run with a larger time step to give damped, quasi-steady solutions for a certain phenomenon if it is known a priori that this particular phenomenon has an insignificant effect on the total system simulation. The present scheme used in the RELAP5 thermal-hydraulic system code [4, 10] is based upon the above concepts. The interphase transfer processes are evaluated implicitly, as are the terms responsible for the fast acoustic pressure wave phenomena. In many simulations, the energy associated with acoustic phenomena is known a priori to be small, and the

TABLE I

Accurate Wavelength versus Courant Number

$u(\Delta t/\Delta x)$	0.1	1	10	100
λ (m)	1.00	11.00	110.00	1102.00

numerical simulation is carried out with a time step much larger then the acoustic Courant limit. When this is done, the acoustic waves and reflections are not simulated but are effectively filtered out by the calculations. Since these waves do not have a significant effect on the mass and energy inventory, the resulting speedup in run time obtained with the larger Δt is very desirable.

The present semi-implicit numerical scheme used in the RELAP5 code is stable for time steps corresponding to a material Courant number less than unity ($\Delta t < \Delta x/v$, where v is of the order of the phasic velocities). This limitation is a result of the explicit evaluation of the properties associated with convective processes. If the convected properties were evaluated implicitly, then a time step corresponding to a material Courant number greater than one could be used. An important question relative to calculations for a Courant number greater than unity is: What processes will be accurately simulated? The simple example previously presented indicated that all dynamically propagating spatial gradients related to acoustic, kinematic, and energy propagation will, in this case, be filtered out by the numerical process. If the dynamic propagation processes present in the differential model are filtered out by the numerical solution process and all the implicit source terms assume their asymptotic steady-state values, then the numerical response is simply a quasi-steady response to the time-varying boundary conditions and/or source terms. If the boundary conditions and prescribed source terms in two-phase flows systems (these correspond to heat addition/removal and pumps) vary slowly, the quasi-steady response reflected in the numerical simulation will represent the dominant physics of interest. In this case, the magnitude of the time step used must be appropriate to the quasi-steady phenomena of interest and the rate of variation of the boundary/source conditions.

4. The Nearly-Implicit Scheme

For problems where the flow is expected to change very slowly with time, it is possible to obtain adequate information from an approximate solution based on very large time steps. This would be advantageous if a reliable and efficient means could be found for solving difference equations treating all terms—phase exchanges, pressure propagation, and convection—by implicit differences. Unfortunately, the state of the art is less satisfactory here than in the case of semi-implicit (convection-explicit) schemes. A fully-implicit scheme for the six-equation model for a 100-cell problem would require the solution of 600 coupled algebraic equations. If these equations were linearized for a straight pipe, inversion of a block tri-diagonal 600×600 matrix with 6×6 blocks would be required. The recent reference [8] describes a numerical scheme that comes very close to this fully-implicit evaluation of all terms.

To avoid a frontal assault on the problem of solving fully-implicit difference schemes, fractional step (sometimes called multiple step) methods have been tried [11]. The equations can be split into fractional steps based upon physical

phenomena. This is the basic idea in the development of the nearly-implicit scheme. Fractional step methods for two-phase flow problems have been developed in Refs [7, 5]. These earlier efforts have been used to guide the present development. The fractional step method developed here differs from that in Ref. [5] in the reduced number of steps used to evaluate the momentum equations.

The nearly-implicit scheme consists of a first step that solves all six conservation equations, treating all interphase exchange processes, the pressure propagation process, and the *momentum* convection process implicity. This step uses the finite difference equations recorded below. Figure 1 defines the index structure used for the staggered grid.

The vapor density equation is

$$\alpha^n_{g,L}(\tilde{\rho}^{n+1}_{g,L}-\rho^n_{g,L})+\rho^n_{g,L}(\tilde{\alpha}^{n+1}_{g,L}-\alpha^n_{g,L}) + (\dot{\alpha}^n_{g,j+1}\dot{\rho}^n_{g,j+1}v^{n+1}_{g,j+1}-\dot{\alpha}^n_{g,j}\dot{\rho}^n_{g,j}v^{n+1}_{g,j})\,\Delta t/\Delta x=\tilde{\Gamma}^{n+1}_{g,L}\,\Delta t \tag{17}$$

and the liquid density equation is

$$\alpha^n_{f,L}(\tilde{\rho}^{n+1}_{f,L}-\rho^n_{f,L})-\rho^n_{f,L}(\tilde{\alpha}^{n+1}_{g,L}-\alpha^n_{g,L}) + (\dot{\alpha}^n_{f,j+1}\dot{\rho}^n_{f,j+1}v^{n+1}_{f,j+1}-\dot{\alpha}^n_{f,j}\dot{\rho}^n_{f,j}v^{n+1}_{f,j})\,\Delta t/\Delta x=-\tilde{\Gamma}^{n+1}_{g,L}\,\Delta t \tag{18}$$

where

$$\tilde{\Gamma}^{n+1}_{g,L}=-\left(\frac{1}{h^*_g-h^*_f}\right)^n_L[H^n_{ig,L}(\tilde{T}^{s,n+1}_L-\tilde{T}^{n+1}_{g,L}) + H^n_{if,L}(\tilde{T}^{s,n+1}_L-\tilde{T}^{n+1}_{f,L})]. \tag{19}$$

The vapor energy equation is

$$(\rho^n_{g,L}U^n_{g,L}+P^n_L)(\tilde{\alpha}^{n+1}_{g,L}-\alpha^n_{g,L})+\alpha^n_{g,L}U^n_{g,L}(\tilde{\rho}^{n+1}_{g,L}-\rho^n_{g,L}) + \alpha^n_{g,L}\rho^n_{g,L}(\tilde{U}^{n+1}_{g,L}-U^n_{g,L})+[\dot{\alpha}^n_{g,j+1}(\dot{\rho}^n_{g,j+1}\dot{U}^n_{g,j+1}+P^n_L)v^{n+1}_{g,j+1} - \dot{\alpha}^n_{g,j}(\dot{\rho}^n_{g,j}\dot{U}^n_{g,j}+P^n_L)v^{n+1}_{g,j}]\,\Delta t/\Delta x=\left[-\left(\frac{h^*_f}{h^*_g-h^*_f}\right)^n_L H^n_{ig,L}(\tilde{T}^{s,n+1}_L-\tilde{T}^{n+1}_{g,L} - \left(\frac{h^*_g}{h^*_g-h^*_f}\right)^n_L H^n_{if,L}(\tilde{T}^{s,n+1}_L-\tilde{T}^{n+1}_{f,L})+Q^n_{wg,L}\right]\Delta t. \tag{20}$$

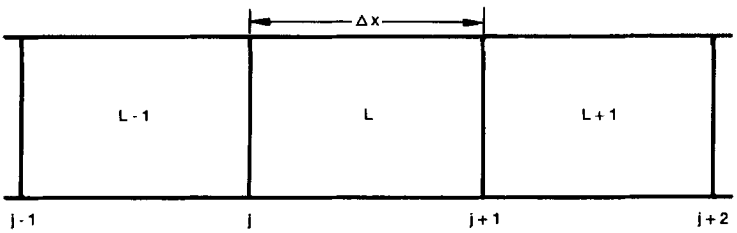

FIG. 1. Typical cell structure.

The liquid energy equation is

$$
\begin{aligned}
&-(\rho^n_{f,L} U^n_{f,L} + P^n_L)(\tilde{\alpha}^{n+1}_{g,L} - \alpha^n_{g,L}) + \alpha^n_{f,L} U^n_{f,L}(\tilde{\rho}^{n+1}_{f,L} - \rho^n_{f,L}) \\
&+ \alpha^n_{f,L}\rho^n_{f,L}(\tilde{U}^{n+1}_{f,L} - U^n_{f,L}) + [\dot{\alpha}^n_{f,j+1}(\dot{\rho}^n_{f,j+1}\dot{U}^n_{f,j+1} + P^n_L)\, v^{n+1}_{f,j+1} \\
&- \dot{\alpha}^n_{f,j}(\dot{\rho}^n_{f,j}\dot{U}^n_{f,j} + P^n_L)\, v^{n+1}_{f,j}] \, \Delta t/\Delta x = \left[\left(\frac{h^*_f}{h^*_g - h^*_f}\right)^n_L H^n_{ig,L}(\tilde{T}^{s,n+1}_L - \tilde{T}^{n+1}_{g,L}) \right. \\
&\left. + \left(\frac{h^*_g}{h^*_g - h^*_f}\right)^n_L H^n_{if,L}(\tilde{T}^{s,n+1}_L - \tilde{T}^{n+1}_{f,L}) + Q^n_{wf,L}\right] \Delta t. \qquad (21)
\end{aligned}
$$

The sum and difference momentum equations are

$$
\begin{aligned}
&(\alpha_g\rho_g)^n_j\,(v^{n+1}_g - v^n_g)_j\,\Delta x_j + (\alpha_f\rho_f)^n_j\,(v^{n+1}_f - v^n_f)_j\,\Delta x_j \\
&\quad + \tfrac{1}{2}(\dot{\alpha}_g\dot{\rho}_g)^n_j[(v^n_{g,L})^2 + 2\,v^n_{g,L}(v^{n+1}_{g,L} - v^n_{g,L}) - (v^n_{g,L-1})^2 \\
&\quad - 2\,v^n_{g,L-1}(v^{n+1}_{g,L-1} - v^n_{g,L-1})]\,\Delta t + \tfrac{1}{2}(\dot{\alpha}_f\dot{\rho}_f)^n_j[(v^n_{f,L})^2 \\
&\quad + 2\,v^n_{f,L}(v^{n+1}_{f,L} - v^n_{f,L}) - (v^n_{f,L-1})^2 - 2\,v^n_{f,L-1}(v^{n+1}_{f,L-1} - v^n_{f,L-1})]\,\Delta t \\
&= -(P_L - P_{L-1})^{n+1}\Delta t + [\rho^n_j B - (\alpha_g\rho_g)^n_j F^n_{wg,j}(v_g)^{n+1}_j \\
&\quad - (\alpha_f\rho_f)^n_j F^n_{wf,j}(v_f)^{n+1}_j]\,\Delta x_j \Delta t \qquad (22)
\end{aligned}
$$

and

$$
\begin{aligned}
&[(v^{n+1}_g - v^n_g)_j - (v^{n+1}_f - v^n_f)_j]\,\Delta x_j \\
&\quad + \tfrac{1}{2}[(\dot{\alpha}_g\dot{\rho}_g)/(\alpha_g\rho_g)]^n_j[(v^n_g)^2_L + 2\,v^n_{g,L}(v^{n+1}_{g,L} - v^n_{g,L}) - (v^n_{g,L-1})^2 \\
&\quad - 2\,v^n_{g,L-1}(v^{n+1}_{g,L-1} - v^n_{g,L-1})]\,\Delta t - \tfrac{1}{2}[(\dot{\alpha}_f\dot{\rho}_f)/(\alpha_f\rho_f)]^n_j[(v^n_{f,L})^2 \\
&\quad + 2\,v^n_{f,L}(v^{n+1}_{f,L} - v^n_{f,L}) - (v^n_{f,L-1})^2 - 2\,v^n_{f,L-1}(v^{n+1}_{f,L-1} - v^n_{f,L-1})]\,\Delta t \\
&= -[(\rho_f - \rho_g)/(\rho_g\rho_f)]^n_j(P_L - P_{L-1})^{n+1}\Delta t - [F^n_{wg,j}(v_g)^{n+1}_j - F^n_{wf,j}(v_f)^{n+1}_j \\
&\quad + (\rho F_i)^n_j(v_g - v_f)^{n+1}_j]\,\Delta x_j \Delta t. \qquad (23)
\end{aligned}
$$

In the above difference equations, a superposed dot denotes a donor cell variable, and a tilde value denotes an intermediate variable that will be reevaluated on the second step. The variables $\tilde{T}^{n+1}_g$, $\tilde{T}^{n+1}_f$, and $\tilde{T}^{s,n+1}$ are obtained from a linearized state equation as functions of $(\tilde{U}^{n+1}_g, P^{n+1})$, $(\tilde{U}^{n+1}_f, P^{n+1})$, and P^{n+1}, respectively.

These finite difference equations are *exactly* those solved in the semi-implicit scheme, with one major change. The convective terms in the momentum Eqs. (22) and (23) are evaluated implicitly (in a linearized form) instead of in an explicit donored fashion as is done in the semi-implicit scheme.

Although this additional implicitness involves only the momentum convective terms, it has a large impact on the algebraic solution algorithm in the first step. In

the semi-implicit scheme, Eqs. (17) through (21) can be solved locally to give a single equation of the form

$$P_L^{n+1} = A\, v_{g,j+1}^{n+1} + B\, v_{g,j}^{n+1} + C\, v_{f,j+1}^{n+1} + D\, v_{f,j}^{n+1} + E \tag{24}$$

for pressure where A, B, C, D, and E contain old time variables only (see Fig. 1 for cell indexes).

In the semi-implicit scheme, the momentum equations can also be solved locally to obtain

$$v_{g,j}^{n+1} = A^1(P_L^{n+1} - P_{L-1}^{n+1}) + C^1 \tag{25}$$

and

$$v_{f,j}^{n+1} = B^1(P_L^{n+1} - P_{L-1}^{n+1}) + D^1 \tag{26}$$

where A^1, B^1, C^1, and D^1 again contain only n level variables. If the momentum Eqs. (25) and (26) are used to eliminate $n+1$ level velocities from Eq. (24), we get the normal pressure equation used in the semi-implicit scheme to obtain all the $n+1$ pressures. For a 100-cell straight pipe problem, this results in a 100×100 tri-diagonal matrix system to solve for all the P^{n+1}.

In the new scheme, because the momentum flux terms are implicit, the momen-

through (21) can still be used to obtain Eq. (24). Equation (24) is then used to eliminate the $n+1$ level pressure terms from Eqs. (22) and (23). A coupled pair of momentum equations involving only $n+1$ level velocities is obtained. Because of the $n+1$ level flux terms, this is a globally coupled system. For a straight pipe of 100 junctions, a block tri-diagonal matrix system 200×200 with 2×2 blocks is obtained. This system is solved using a sparse matrix solution algorithm. Once the v_f^{n+1} and v_g^{n+1} solution is obtained, P^{n+1} is obtained by back substitution into Eq. (24). Using Eqs. (17) through (21), intermediate/provisional $n+1$ values for α_g, U_g, and U_f, denoted by $\tilde{\alpha}_g^{n+1}$, $\tilde{U}_g^{n+1}$, and $\tilde{U}_f^{n+1}$, can also be obtained. (By way of contrast, this single step replaces three steps used in the SETS scheme [5]—the pre-prediction step for velocities, the velocity convection stabilization step, and the semi-implicit step involving implicit pressures.)

The second step in the nearly-implicit scheme is used to stabilize the convective terms in the mass and energy balance equations. This step uses the final $n+1$ level velocities from the first step along with the interphase exchange terms resulting from the first step, i.e., the interphase heat and mass exchanges for step 2 are calculated using P^{n+1}, $\tilde{U}_g^{n+1}$, and $\tilde{U}_f^{n+1}$ from step 1. The phasic continuity and energy equations in this second step have the fluxed variables evaluated at the $n+1$ time level, i.e., implicity as compared to their explicit evaluation in the first step.

The vapor density equation is

$$(\alpha_g\rho_g)_L^{n+1} - (\alpha_g\rho_g)_L^n + [(\dot{\alpha\rho})_{g,j+1}^{n+1} v_{g,j+1}^{n+1} - (\dot{\alpha\rho})_{g,j}^{n+1} v_{g,j}^{n+1}]\,\Delta t/\Delta x = \tilde{\Gamma}_{g,L}^{n+1}\,\Delta t. \tag{27}$$

The liquid density equation is

$$(\alpha_f\rho_f)_L^{n+1} - (\alpha_f\rho_f)_L^n + [(\dot{\alpha\rho})_{f,j+1}^{n+1} v_{f,j+1}^{n+1} - (\dot{\alpha\rho})_{f,j}^{n+1} v_{f,j}^{n+1}]\,\Delta t/\Delta x = -\tilde{\Gamma}_{g,L}^{n+1}\,\Delta t. \tag{28}$$

In these continuity equations, the mass exchange $\tilde{\Gamma}_g^{n+1}$ is evaluated using the provisional values from the first step [see Eq. (19)].

The vapor energy equation is given by

$$\begin{aligned}(\alpha_g\rho_g U_g)_L^{n+1} - (\alpha_g\rho_g U_g)_L^n + [(\alpha\dot{\rho}U)_{g,j+1}^{n+1} v_{g,j+1}^{n+1} - (\alpha\dot{\rho}U)_{g,j}^{n+1} v_{g,j}^{n+1}]\,\Delta t/\Delta x \\ = -P_L^n(\tilde{\alpha}_{g,L}^{n+1} - \alpha_{g,L}^n) - P_L^n(\dot{\alpha}_{g,j+1}^n v_{g,j+1}^{n+1} - \dot{\alpha}_{g,j}^n v_{g,j}^{n+1})\,\Delta t/\Delta x \\ + \left[-\left(\frac{h_f^*}{h_g^* - h_f^*}\right)_L^n H_{ig,L}^n (\tilde{T}_L^{s,n+1} - \tilde{T}_{g,L}^{n+1}) \right. \\ \left. - \left(\frac{h_g^*}{h_g^* - h_f^*}\right)_L^n H_{if,L}^n (\tilde{T}_L^{s,n+1} - \tilde{T}_{f,L}^{n+1}) + Q_{wg,L}^n \right] \Delta t.\end{aligned} \tag{29}$$

The liquid energy equation is given by

$$\begin{aligned}(\alpha_f\alpha_f U_f)_L^{n+1} - (\alpha_f\rho_f U_f)_L^n + [(\alpha\dot{\rho}U)_{f,j+1}^{n+1} v_{f,j+1}^{n+1} - (\alpha\dot{\rho}U)_{f,j}^{n+1} v_{f,j}^{n+1}]\,\Delta t/\Delta x \\ = P_L^n(\tilde{\alpha}_{g,L}^{n+1} - \alpha_{g,L}^n) - P_L^n(\dot{\alpha}_{f,j+1}^n v_{f,j+1}^{n+1} - \dot{\alpha}_{f,j}^n v_{f,j}^{n+1})\,\Delta t/\Delta x \\ + \left[\left(\frac{h_f^*}{h_g^* - h_f^*}\right)_L^n H_{ig,L}^n (\tilde{T}_L^{s,n+1} - \tilde{T}_{g,L}^{n+1}) \right. \\ \left. + \left(\frac{h_g^*}{h_g^* - h_f^*}\right)_L^n H_{if,L}^n (\tilde{T}_L^{s,n+1} - \tilde{T}_{f,L}^{n+1}) + Q_{wf,L}^n \right] \Delta t.\end{aligned} \tag{30}$$

This second step uses the mass and energy balance equations only. If the structure of Eqs. (27) through (30) is examined, it is seen that each equation only involves one unknown variable: Eq. (27)—$(\alpha\rho)_g^{n+1}$, Eq. (28)—$(\alpha\rho)_f^{n+1}$, Eq. (29)—$(\alpha\rho U)_g^{n+1}$, and Eq. (30)—$(\alpha\rho U)_f^{n+1}$.

This is because the new time velocities, v_g^{n+1} and v_f^{n+1}, are known from step 1 and provisional $n+1$ values from step 1 are used in the exchange terms. Hence each equation is uncoupled from the other and can be solved independently. In addition, the two equations involving the gas phase, Eqs. (27) and (29), have the same structural form for the convective terms; i.e., each equation convects with velocity v_g^{n+1}. The matrix multiplying the unknown new time variable in Eq. (27) is decomposed only once, and then this decomposition is used with different right-hand sides to

solve both Eqs. (27) and (29). Hence for a straight pipe problem of 100 cells, only one 100×100 tri-diagonal system must be decomposed to obtain $(\alpha\rho)_g^{n+1}$ and $(\alpha\rho U)_g^{n+1}$. In like manner, the liquid phase Eqs. (28) and (30) have the same structure and require only one decomposition to be carried out to solve both equation sets, giving $(\alpha\rho)_f^{n+1}$ and $(\alpha\rho U)_f^{n+1}$.

With the above four new variables known, we obtain U_g^{n+1}, U_f^{n+1}, and α_f^{n+1} as

$$U_g^{n+1} = (\alpha\rho U)_g^{n+1}/(\alpha\rho)_g^{n+1}, \tag{31}$$

$$U_f^{n+1} = (\alpha\rho U)_f^{n+1}/(\alpha\rho)_f^{n+1}, \tag{32}$$

and

$$\alpha_f^{n+1} = (\alpha\rho)_f^{n+1}/\rho_f^{n+1}, \tag{33}$$

where ρ_f^{n+1} is the liquid density calculated from the linearized state relationship using U_f^{n+1} and P^{n+1}. If any phase vanishes, so that $(\alpha\rho)^{n+1}$ equals zero, the provisional $n+1$ value of the corresponding variable is used to avoid the zero divisor in Eqs. (31) and (32). Equation (33) was chosen to obtain α_f^{n+1} because the liquid phase is nearly incompressible, and less void error is expected using the liquid mass balance.

This second step stabilizes the convective terms in the mass and energy equations, and it does so with very little computational effort because of the fractional step nature of the scheme. A detailed comparison of the calculation times for the nearly-implicit method, the SETS method, and the recently described method used in the ATHENA code will be presented in Section 6.

An observation concerning steady state should be noted. In steady state, the difference between $n+1$ level variables and n level variables disappears, and the nearly-implicit scheme gives the same solution as the semi-implicit scheme, except for minor variations caused by the momentum flux terms. The momentum flux terms use a donor cell formulation in the semi-implicit scheme, whereas the nearly-implicit scheme uses a centered formulation. In our experience, the difference at steady state has been less than 1%.

5. Some Accuracy Considerations

The first step of the nearly-implicit scheme has an accuracy very close to that of the semi-implicit scheme. The only difference between the two is the implicitly evaluated momentum convective terms.

The accuracy of the second step will be examined in this section, using the simple model of Eq. (13). This model is considered for a numerical scheme parallel to that used for a mass or energy equation in the nearly-implicit scheme. Consider a

scheme in which the source terms are evaluated implicitly on the first step and the convective terms are evaluated implicitly on the second step: First step:

$$\tilde{a}_j^{n+1} - a_j^n + \frac{u\,\Delta t}{2\,\Delta x}(a_{j+1}^n - a_{j-1}^n) = -\frac{\Delta t}{\tau}\tilde{a}_j^{n+1}. \tag{34}$$

Second step:

$$a_j^{n+1} - a_j^n + \frac{u\,\Delta t}{2\,\Delta x}(a_{j+1}^{n+1} - a_{j-1}^{n+1}) = -\frac{\Delta t}{\tau}\tilde{a}_j^{n+1}. \tag{35}$$

Assuming an infinite medium and a general Fourier solution component, the first step gives for $\tilde{a}_j^{n+1}$

$$\tilde{a}_j^{n+1} = \left[\frac{1 - i(u\,\Delta t/\Delta x)\sin(k\,\Delta x)}{1 + \Delta t/\tau}\right] a_j^n. \tag{36}$$

The second step gives the final Fourier solution component a_j^{n+1}

$$a_j^{n+1} = \frac{a_j^n - (\Delta t/\tau)\,\tilde{a}_j^{n+1}}{1 + i(u\,\Delta t/\Delta x)\sin(k\,\Delta x)} \tag{37}$$

or

$$a_j^{n+1} = \left[\frac{\left[1 - \left(\frac{\Delta t}{\tau}\right)\frac{1 - i(u\,\Delta t/\Delta x)\sin(k\,\Delta x)}{1 + \Delta t/\tau}\right]}{1 + i(u\,\Delta t/\Delta x)\sin(k\,\Delta x)}\right] a_j^n. \tag{38}$$

Equation (38) yields an amplification factor of absolute value less than unity for any time step; hence the scheme is unconditionally stable. For large times steps such that $\Delta t/\tau \gg 1$ and $(u\,\Delta t/\Delta x)\sin(k\,\Delta x) > 1$ (i.e., both are large but $\Delta t/\tau \gg (u\,\Delta t/\Delta x)\sin(k\,\Delta x)$), Eq. (38) reduces to

$$a_j^{n+1} \approx a_j^n. \tag{39}$$

The implicit two-step method, Eqs. (34) and (35), gives a solution for a_j^{n+1} that is basically unchanged from that at the nth time level. Hence, although the scheme in Eqs. (34) and (35) is unconditionally stable, it is extremely inaccurate for large time steps. For large time steps the model [Eq. (13)] has solutions that decay to zero.

The source of the inaccuracy is easily seen from an examination of Eqs. (36) and (37). Equation (36) shows that the provisional new time value $\tilde{a}_j^{n+1}$ is approximately zero. This is the proper asymptotic large-time value and is attained because the first step has the source term evaluated implicitly. The second step, Eq. (37), now magnifies small $\tilde{a}_j^{n+1}$ and gives $a_j^{n+1} \simeq a_j^n$. The magnification in the

second step is due to the explicit evaluation of the source term (corresponding to the interphase mass and heat exchange terms) in the second step. This "frozen" evaluation of the exchange process causes the second step to take place as if there were no feedback between the mass transfer and convective process. Thus, the implicit convective process in the second step can give a resulting solution that has a very inaccurate calculation for the mass transfer. This inaccuracy will be seen in Section 6 with a specific test problem. The potential for inaccuracies in fractional step methods has been previously mentioned (see Ref. [12]).

6. Model Development Test Problems

This section describes three simple problems that were used to give a preliminary indication of the general features, both positive and negative, of the nearly-implicit scheme.

The format for presentation of each problem will be (a) description, (b) purpose of calculation, (c) results, and (d) conclusions. Each problem was run using steam/water properties for the state relationships.

6.1. *Problem* 1: *Water Faucet*

This is a conceptual problem using a straight vertical pipe of 12 volumes (each 1 m in length). All profiles are initially uniform, with a liquid velocity of 10 m/s, a vapor velocity of 0 m/s, a pressure of 1×10^6 Pa, and a vapor void fraction of 0.205. The inlet boundary conditions keep the inlet velocities and void fraction at their initial values. The calculation is carried out until a steady flow is attained.

This problem was run with the interphase exhange of mass set to zero and zero interphase drag. For this situation, the problem has the analytical steady-state solution developed below. This analytical solution was first used as a code test problem in Ref. [13].

At this pressure the vapor density is 0.0056 times the liquid density; therefore, the pressure gradient in the vapor (and hence liquid) is approximately zero. With this uniform pressure, the steady-state liquid momentum equation reduces to

$$\alpha_f \rho_f v_f \frac{\partial v_f}{\partial x} = \alpha_f \rho_f g \tag{40}$$

which can be directly integrated from the inlet to an arbitrary x (measured from the inlet) to obtain

$$\tfrac{1}{2}\rho_f v_f^2 |_x = \tfrac{1}{2}\rho_f v_f^2 |_{\text{inlet}} + \rho_f g x. \tag{41}$$

Since the liquid is nearly incompressible, Eq. (41) gives the liquid velocity at section x. The steady-state mass balance for the liquid gives

$$\frac{\partial(\alpha_f v_f)}{\partial x} = 0 \tag{42}$$

or

$$\alpha_f|_x = \frac{\alpha_f v_f|_{\text{inlet}}}{v_f|_x}. \tag{43}$$

If v_g equals zero and the liquid and vapor entropies remain fixed at their initial values, then Eqs. (41) and (43) give the exact steady-state solution. An examination

state necking/contracting profile is dynamically approached by means of a void fraction wave propagating down the pipe. The major purpose of this test problem was to show how the nearly-implicit scheme filters out dynamic kinematic waves when run with a time step larger than the material Courant time step.

A base case was run with the semi-implicit scheme using a time step $\Delta t = 0.025$ s, which is approximately one-half the material Courant limit. The void fraction as a function of time is shown in Fig. 2 for the top five cells. This figure shows the dynamic propagation of the void profile down the pipe until the wave has completely passed out of the pipe and the steady-state profile remains. This semi-implicit simulation took 84 steps to reach steady state.

The same problem was then run using the nearly-implicit scheme. This simulation was carried out with a time step $\Delta t = 10$ s, which is ~ 150 times the material Courant limit. The final steady state is also shown in Fig. 2, and it is the same as that for the semi-implicit scheme. The nearly-implicit simulation took seven steps to reach steady state. The nearly-implicit scheme reached steady state 5.9 times faster (CPU time) than the semi-implicit scheme.

The grind time for the nearly-implicit scheme is ~ 0.0024 CPU s/cell/time step on the CDC 176. This is ~ 1.6 times the grind time of the semi-implicit scheme. This grind time increase is characteristic of all problems. It is caused by the larger matrix solution required for the nearly-implicit velocity calculation and the additional matrix solutions required in the second implicit convective step.

The computational efficiency of the nearly-implicit scheme can easily be compared with the two other Courant violating numerical schemes. The computational efficiency for the SETS scheme [5] and the scheme used in ATHENA [8] is taken from Ref. [8]. All quoted node cycle times, or CPU time/time step/node, are for the CDC Cyber 175.[1] For straight pipe test problems, the node cycle times are (i) 0.0060 s for the nearly-implicit scheme, (ii) 0.0060 s for the SETS scheme, and (iii) 0.0095 s for the ATHENA scheme.[2] It should be noted that the SETS scheme is the

[1] In some cases, a conversion from run times reported on a CDC Cyber 176 was needed. The CDC Cyber 175 is approximately 2.5 times slower than the CDC Cyber 176 [8]. This conversion factor was used whenever necessary.

[2] In Ref. [8], two different straight pipe test problems were run, and this node cycle time is the average for these two test cases.

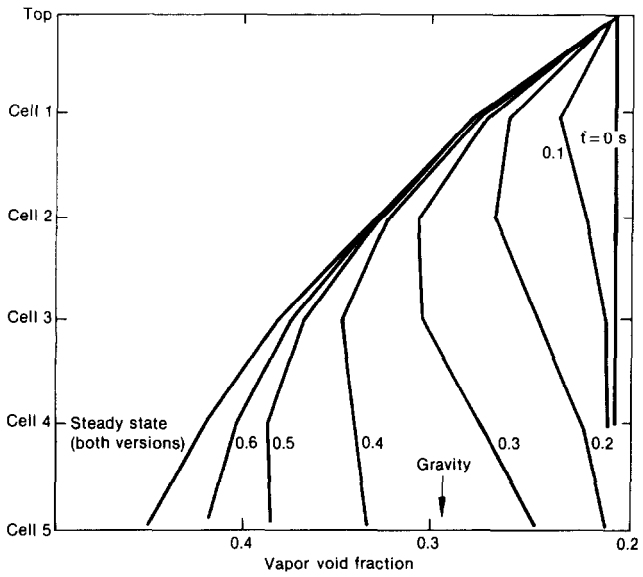

FIG. 2. Transient vapor void profile.

least implicit of the three schemes and the ATHENA scheme is the most implicit. The nearly-implicit scheme and the SETS scheme have comparable node cycle times. The ATHENA scheme has a somewhat larger node cycle time. Presumably, this is due to the larger size blocks that appear in the block triangular matrix that must be decomposed.

Both the semi-implicit and nearly-implicit runs reached a steady state that was within 1% of the approximate analytical solution developed above.

The filteriing characteristic of the nearly-implicit scheme is clearly evident in this calculation. As shown in Fig.2, the semi-implicit calculation uses a time step small enough to follow the dynamic motion of the void fraction profile as it propagates down the pipe.

The nearly-implicit scheme when used with the large time step above gave a void profile that after *one* step was within 3% of the steady state profile in every cell; i.e., no dynamic propagation was calculated but only the steady-state profile. This characteristic of an implicit scheme is consistent with the earlier theoretical model analysis in Section 3.

6.2. *Problem 2: Heated Pipe*

This simulation used a straight horizontal pipe of 12 volumes. The pipe inlet boundary conditions consisted of an influx of pure liquid with a flow rate of 0.43907 kg/s at saturation conditions with a temperature of 530 K. The pipe wall was simulated with 12 heat slabs each with six temperatures nodes initially also at 530 K. The outside of the pipe was subjected to a heat flux ramp that went from 0

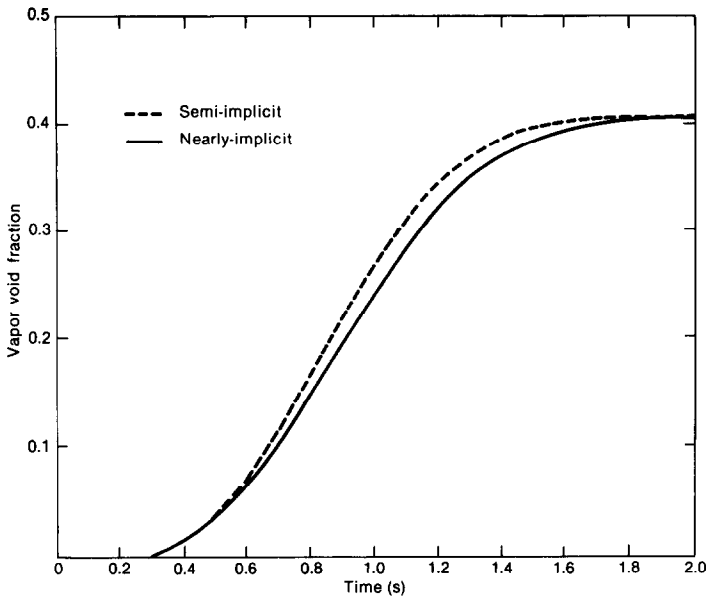

FIG. 3. Vapor void fraction at cell 12—ramp heat flux.

to 3×10^5 W/m^2 in 1 s and then remained constant. This external wall heat flux caused the pure liquid to boil as it flowed down the pipe. The transient boiling eventually gave rise to a steady void profile. The total pipe length was 0.762 m, with an outside diameter of 0.025 m.

The purpose of this simulation was to show that if dynamic propagation effects are not significant, then the nearly-implicit scheme can give reasonable simulations of the system as it responds to slowly changing boundary conditions. The heat supplied in this problem gave rise to an equivalent wall heat flux source in the hydrodynamic solution.

As in Problem 1, a base case was run using the semi-implicit scheme. This was used as a reference solution to which the nearly-implicit calculation was compared. Figure 3 shows a comparison of the vapor void fraction calculated in the last cell in the pipe by the two different schemes. Both simulations reach the same steady state after ~ 2 s. The nearly-implicit scheme was run with $\Delta t = 0.1$ s, giving a time step that was form two to three times the material Courant limit. The semi-implicit scheme was run using a Δt that was from three-fourths to one time the material Courant limit. To calculate 3 s of simulated time the semi-implicit scheme took 111 steps. The nearly-implicit scheme took 30 steps. The nearly-implicit scheme reached steady state in about half the computer time required by the semi-implicit scheme.

The vapor void fraction profife for thc nearly-implicit scheme shows the same trend as the reference case, and it remains within 5% of the semi-implicit curve, though always below it. Similar agreement was seen for the velocities.

The nearly-implicit scheme was able to accurately calculate the transient vapor void fraction and velocity profiles caused by an external heat flux. This shows that an implicit scheme can be used to efficiently simulate slow transients.

A remark concerning the run time comparisons between the two schemes should be made. In both Problem 1 and Problem 2, the pipes were composed of only a few (12) cells. In system–type calculations the number of cells is greatly increased. It is expected that the semi-implicit scheme, being limited by a material Courant number of one, will run even longer relative to the nearly-implicit scheme in these problems because of the increased transport time for flow around the system. In these short pipe problems the time required by the semi-implicit scheme is minimized because of the short transport time for flow through the pipe.

6.3. *Problem* 3: *Fast Transient Blowdown*

This problem was a straight pipe blowdown of a low-quality mixture. The initial conditions were saturated fluid at 7×10^6 Pa, with a vapor void fraction of 4.8×10^{-2}. The pipe consisted of 12 cells and was 2.46 m long. It was blown down to atmospheric pressure.

The purpose of the simulation was to show the inefficiency of the nearly-implicit scheme for fast transients.

This calculation, as in the previous problems, was run using both semi-implicit and nearly-implicit schemes. Both runs gave similar pressure and void transients.

Figure 4 shows the pressure transient in volume 6 for both schemes. Both simulations were controlled by the built-in mass error time step control in RELAP5/MOD2. Both schemes took 0.2 s to blow down to atmospheric pressure.

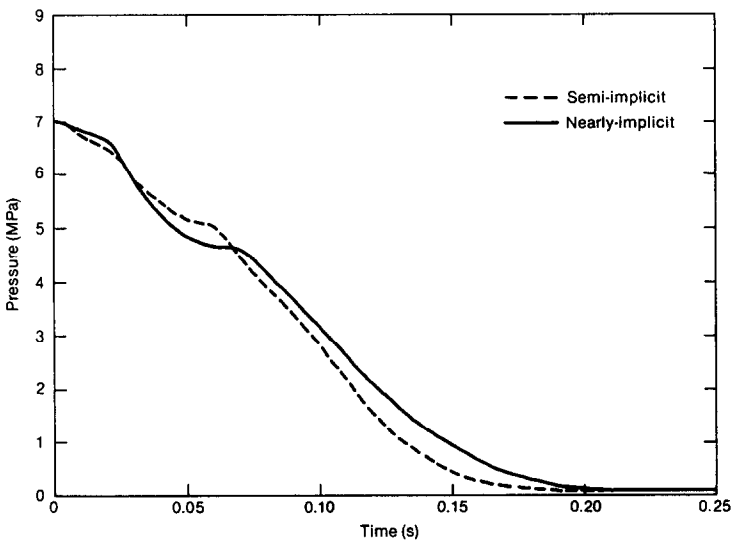

FIG. 4. Pressure plots in volume 6 for the fast transient flowdown problem.

The semi-implicit scheme took 120 steps to blow down. The nearly-implicit scheme took 41 steps to blow down. The nearly-implicit simulation took about half the computer time required by the semi-implicit simulation.

A brief comment concerning the semi-implicit results is in order. The blowdown proceeds as expected except for a flattening of the pressure profile around 0.06 s. This is due to the increased mass transfer rate between the phases when the depressurization wave reaches the closed end of the pipe. A convergence study with the semi-implicit scheme clearly shows this to be physical and not numerical. Although the nearly-implicit scheme took time steps on the average three times larger than those of the semi-implicit scheme, the plots clearly show inaccuracies associated with these larger times steps. A convergence study using the nearly-implicit scheme shows that for smaller time steps, the nearly-implicit scheme converges to the semi-implicit scheme result. The inaccuracies exhibited by the nearly-implicit scheme using the larger time step clearly show that this scheme is inefficient for the simulation of this fast transient. In this simulation, the important point is to accurately calculate the mass transfer rates as these govern the depressurization. Although the nearly-implicit scheme has a Courant violating time step with no stability problem the mass transfer rate is not accurately simulated at these larger time steps.

7. Conclusions

This paper presents a description and test results for the new nearly-implicit hydrodynamic numerical scheme that has been implemented in the RELAP5 thermal-hydraulic system code. Some specific conclusions obtained are as follows:

1. Preliminary analysis indicates that the material Courant limit can be

phenomena.

2. The nearly-implicit method requires less computational time than a fully-implicit method.

3. The explicit evaluation of the source term in the second step results in some inaccuracies. An improved time step controller could be developed to minimize these inaccuracies. Methods of making the source term implicit in the second step may mitigate these inaccuracies.

4. The accurate simulation of the steady state and transient void, velocity, and temperature profiles in the heated pipe problem shows that the scheme can be used to efficiently simulate slow transients.

5. The semi-implicit scheme is a more efficient scheme to use for the simulation of fast transients, as seen from the fast transient blowdown problem.

ACKNOWLEDGMENT

We thank Richard J. Wagner for the work he did in altering the RELAP5 program structure so that this scheme could be implemented.

REFERENCES

1. D. R. LILES *et al.*, Los Alamos National Laboratory Report No. 8709-MS, NUREG/CR-2054, 1981 (unpublished).
2. D. D. TAYLOR *et al.*, Idaho National Engineering Laboratory Report No. EGG-2294, NUREG/CR-3633, 1985 (unpublished).
3. J. H. MCFADDEN *et al.*, Electric Power Research Institute Report No. NP-1850-CCM, 1982 (unpublished).
4. V. H. RANSOM *et al.*, Idaho National Engineering Laboratory Report No. EGG-2396, NUREG/CR-4312, 1985 (unpublished).
5. J. H. MAHAFFY, *J. Comput. Phys.* **46**, 329 (1982).
6. D. R. LILES *et al.*, Los Alamos National Laboratory Report No. LA-9944-MS, NUREG/CR-3567, 1984 (unpublished).
7. H. B. STEWART, *J. Comput. Phys.* **40**, 77 (1981).
8. B. N. HANNA, N. HOBSON, AND D. J. RICHARDS, *American Nuclear Society Proceedings of the* 1985 *National Heat Transfer Conference, Denver, Colorado, August* 1985 (*Amer. Nuclear Soc.*, 1985), p. 119.
9. M. ISHII, *Thermal-Fluid Dynamic Theory of Two-Phase Flow* (*Eyrolles, Paris*, 1975).
10. V. H. RANSOM *et al.*, Idaho National Engineering Laboratory Report No. EGG-2070, NUREG/CR-1826, 1982 (unpublished).
11. N. N. YANENKO, *The Method of Fractional Steps* (Springer–Verlag, New York, 1971).
12. H. B. STEWART AND B. WENDROFF, *J. Comput. Phys.* **56**, 363 (1984).
13. J. H. MCFADDEN, R. W. LYCZKOWSKI, AND G. F. NEDERAUER, Electric Power Research Institute Report, NP-143, 1976 (unpublished).